

Homology modeling and atomic level binding study of *Leishmania* MAPK with inhibitors

Mahendra Awale · Vivek Kumar ·
Parameswaran Saravanan · C. Gopi Mohan

Received: 30 May 2009 / Accepted: 8 July 2009 / Published online: 2 August 2009
© Springer-Verlag 2009

Abstract The current therapy for leishmaniasis is not sufficient and it has two severe drawbacks, host-toxicity and drug resistance. The substantial knowledge of parasite biology is not yet translating into novel drugs for leishmaniasis. Based on this observation, a 3D structural model of *Leishmania* mitogen-activated protein kinase (MAPK) homologue has been developed, for the first time, by homology modeling and molecular dynamics simulation techniques. The model provided clear insight in its structure features, *i.e.* ATP binding pocket, phosphorylation lip, and common docking site. Sequence-structure homology recognition identified *Leishmania* CRK3 (LCRK3) as a distant member of the MAPK superfamily. Multiple sequence alignment and 3D structure model provided the putative ATP binding pocket of *Leishmania* with respect to human ERK2 and LCRK3. This analysis was helpful in identifying the binding sites and molecular function of the *Leishmania* specific MAPK homologue. Molecular docking study was performed on this 3D structural model, using different classes of competitive ATP inhibitors of LCRK3, to check whether they exhibit affinity and could be identified as *Leishmania* MAPK specific inhibitors. It is well known that MAP kinases are extracellular signal regulated kinases

ERK1 and ERK2, which are components of the Ras-MAPK signal transduction pathway which is complexed with HDAC4 protein, and their inhibition is of significant therapeutic interest in cancer biology. In order to understand the mechanism of action, docking of indirubin class of molecules to the active site of histone deacetylase 4 (HDAC4) protein is performed, and the binding affinity of the protein-ligand interaction was computed. The new structural insights obtained from this study are all consistent with the available experimental data, suggesting that the homology model of the *Leishmania* MAPK and its ligand interaction modes are reasonable. Further the comparative molecular electrostatic potential and cavity depth analysis of *Leishmania* MAPK and human ERK2 suggested several important differences in its ATP binding pocket. Such differences could be exploited in the future for designing *Leishmania* specific MAPK inhibitors.

Keywords Docking · Homology modeling · *Leishmania* CRK3 · *Leishmania* MAPK · Molecular dynamics

Introduction

Leishmaniasis is an infectious disease caused by the protozoan parasites. It is transmitted by the bite of certain species of sand flies. This disease affects mainly in the tropical and subtropical countries, such as India, Bangladesh, Nepal, Afghanistan, Sudan, Saudi Arabia, East and North Africa, rainforests in Central and South America and Brazil. The disease has an estimated global prevalence of 12 million people worldwide, with an average of 1.5–2 million new cases annually [1–4].

There are three clinical forms of leishmaniasis: visceral leishmaniasis (VL), cutaneous leishmaniasis (CL), and

Electronic supplementary material The online version of this article (doi:10.1007/s00894-009-0565-3) contains supplementary material, which is available to authorized users.

M. Awale · V. Kumar · P. Saravanan · C. G. Mohan (✉)
Centre for Pharmacoinformatics,
National Institute of Pharmaceutical
Education and Research (NIPER),
Sector 67, S.A.S. Nagar,
160 062 Punjab, India
e-mail: cmohan@niper.ac.in
e-mail: cgopimohan@yahoo.com

mucocutaneous leishmaniasis (MCL) [5, 6]. Each of them is generally associated with certain species and concrete geographical settings. VL caused by *Leishmania donovani* is fatal if untreated, whereas CL caused by species such as *Leishmania major*, *Leishmania Mexicana*, and *Leishmania panamensis*. MCL is mainly caused by species *Leishmania braziliensis*.

Leishmania parasites have a digenetic life cycle with mammals and sand flies as their hosts [6]. In an invertebrate phlebotomine sand fly host, the parasites proliferate in the promastigote (flagellate) form in the insect gut, whereas in a vertebrate host the protozoa are obligate intracellular parasites in the amastigote (non-motile) form infecting mostly mononuclear phagocytes [7]. The therapeutic arsenal against VL is limited; the available agents with established efficacy are all injectable. The pentavalent antimonials have been recommended for the treatment of leishmaniasis for over 50 years [8]. Other drugs used in the treatment of leishmaniasis include the Diamidine pentamidine and Amphotericin B. Well known antimonial drugs can no longer be used in Northeastern India, because of its resistance, where the incidence of VL is highest. Traditional second-line drugs (Pentamidine and Amphotericin B) are more toxic and difficult to administer. Newer drugs, such as the lipid formulations of Amphotericin B (AmBisome, Amphocil and Abelcet), has been effective in the treatment of VL [9]. Unfortunately, the prohibitive cost of the new formulations of these drugs means that the treatment is unavailable to the majority of patients suffering with leishmaniasis. The first oral medication for leishmaniasis was available with the discovery of miltefosine, but was not fully successful and the drug showed teratogenicity with low therapeutic index. Although this progress in treatments is encouraging, the current therapy for leishmaniasis is not sufficient as it was associated with several drawbacks like host-toxicity, drug resistance *etc.* [10].

In 1997, Martin Wiese identified the *Leishmania mexicana* gene coding for a protein with strong homology to mitogen-activated protein kinase (MAPK) of yeast and higher eukaryotes which is required for the amastigote survival and proliferation in macrophages [3, 11]. MAP kinases are a group of serine/threonine kinases. It is reported that MAPK homologue from *Leishmania mexicana* is involved in the formation and maintenance of the flagellum in the promastigote. A deletion mutant was able to infect host cells, unable to proliferate, but transform to the amastigote morphology. Complementation experiments revealed that the *Leishmania* MAPK is required and is sufficient to restore the infectivity. Therefore, this kinase is crucial for the survival of *Leishmania mexicana* in the infected host by affecting the cell division of the amastigotes. Disease progression is prevented by targeting *Leishmania* MAPK by controlling the proliferation in

amastigotes, and thereby affecting the MAPK signaling pathway causing cell division. Thus *Leishmania* MAPK is an ideal drug target and a specific inhibitor of it would be promising to treat the leishmaniasis [12].

In order to further understand the inhibitor binding sites of the modeled protein, several interesting groups of molecules having LCRK3 *anti-leishmanial* activity were identified, including the indirubins, which were investigated in more detail [13]. These molecules, especially indirubin series, caused growth arrest of the *Leishmania* parasite in culture, and altered DNA content with aberrant morphology, leading to the disruption of the cell cycle control through the intracellular inhibition of cyclin dependent kinase (CDK) [13]. Indirubin, an active ingredient of a traditional Chinese recipe Danggui Longhui Wan, is a potent ATP-competitive CDK inhibitor, and therapeutic interventions targeting CDKs have been stimulated for the treatment of various proliferative diseases, such as cancer, psoriasis, and alopecia [14]. These protein kinases are associated with histone deacetylase4 (HDAC4) and can phosphorylate HDAC4 in cells [13, 15]. Also, it is expected that the protein phosphorylation is important for differentiation and proliferation of *Leishmania* parasite, which is also critical for its development. Protein kinases possess high sequence similarity, and understanding the MAPK signaling cascades is very complicated due to the diverse range of signals utilizing the same MAPK pathways; and further its deregulation leads to various disease states [15]. The activation of this pathway might lead to an increased percentage of cells expressing HDAC4 in the nucleus. It is well known that MAP kinases are extracellular signal regulated kinases ERK1 and ERK2, which are components of the Ras-MAPK signal transduction pathway is complexed with HDAC4 protein, and its inhibition is of significant therapeutic interest [16].

It has been well established that MAP kinases play a crucial role in cancer biology. The significant role of the Ras/Raf/MEK/Erk MAPK signaling pathway, in multiple cellular functions, in amastigotes, underlies the importance of the cascade in oncogenesis, and growth of transformed (cancer) cells. As such the therapeutic target identification in MAPK pathway and its validation has been a focus of intense investigation. Selective inhibition of ERK1 and ERK2, which are mammalian MAP kinases, represents a potential approach for the treatment of cancer and other diseases; however, no selective inhibitors are currently available [17–19]. Dauoti *et al.* recently carried out characterization of a novel MAPK kinase 1/2 inhibitor for cancer therapy by showing its unique mechanism of action [20].

Protein structure prediction is one of the most promising tasks in the computational structural biology program. Most commonly used techniques include *de-novo* or *ab-initio* modeling and comparative protein modeling which again is

divided into homology modeling and protein threading. Homology model of different proteins were carried out and its importance in structure-based drug design is elucidated [21]. William *et al.* recently reported the homology modeling and dynamics of the extracellular domain of rat and human neuronal nicotinic acetylcholine receptor subtypes [22]. Docking and MD simulations of the interaction of the tarantula peptide psalmotoxin-1 with the homology model of the channel protein were performed by Pietra F [23].

In the present study, we carried out homology modeling of *Leishmania* MAPK homologue. This three dimensional (3D) structure model provided for the first time, the *in silico* screening of various small molecules for their MAPK inhibitory activity. Further, we have performed molecular docking, comparative molecular electrostatic potential, and cavity depth analysis on this 3D model, in order to understand its function and other physico-chemical properties. Importance of this study in the Ras-MAPK signal transduction pathway using molecular docking analysis is also carried out.

Material and methods

All computational experiments were carried out using MODELLER8v2, SYBYL7.1, Autodock4 and Discovery Studio2.0 molecular modeling packages on a Sun workstation with Red Hat Enterprise Linux 3 and Silicon Graphics Fuel Workstation with IRIX 6.5 operating system.

Homology modeling

Leishmania MAPK homologue sequence was retrieved from UniProtKB/TrEMBL database (Id: O00872). NCBI-BLASTP search against Protein Data Bank (PDB) using *Leishmania* MAPK as query sequence gave a number of homologous sequences. Among these sequences, human ERK2 (PDB code: 1TVO) was chosen as a best template based on high sequence identity (39%) to model the 3-D structure of the *Leishmania* MAPK. The Blosom62 scoring matrix was selected with a gap penalty of 11 and a gap extension penalty of 1 for the BLASTP analysis. The crystal structure of human ERK2 was solved at a resolution of 2.50 Å which is in complex with the 5-(2-phenylpyrazolo [1,5-a] pyridin-3-yl)-1 h-pyrazolo [3,4-c] pyridazin-3-amine ligand (PDB code: 1TVO) [24].

MODELLER is a computer program that generates 3-D model structures of the proteins and their assemblies by satisfaction of spatial restraints. More generally, the input to the program are the alignment file (PAP/PIR formats), restraints on the spatial structure of the amino acid sequence(s) and ligands to be modeled [25]. Sequence alignment obtained from NCBI-BLASTP was used as an

input to MODELLER8v2 for its model building. The structural information of the first seven residues at the N-terminus is not available in the human ERK2 crystal structure, and therefore not included in the homology model building of *Leishmania* MAPK. Initially, a crude homology model for *Leishmania* MAPK was obtained by using automated model building in MODELLER. Five models were generated among which the one which has the best dope score was selected for further ligand modeling. For modeling ligand, it was assumed that the ligand binding modes are similar in the target and the template protein structure. Accordingly, the ligand is then transferred among target structures keeping their orientation as a restraint for the subsequent modeling process. Having placed the ligand in a near-native orientation into the consensus binding-site of the modeled protein, new models were generated by additionally incorporating information of the ligand. During this modeling process, the ligand is kept fixed in space. Quality of the different 3-D structure homology models with its ligand were assessed using Ramachandran plot in PROCHECK validation package, in order to identify the best ligand supported *Leishmania* MAPK model [26].

Refinement strategy of the *Leishmania* MAPK homology model

The best ligand supported *Leishmania* MAPK homology model was selected on the basis of the PROCHECK validation. The initial model showed problems in the conformation of loop region, which was subjected for loop modeling and further validated using ERRAT plot [27]. ERRAT plot gives the measure of the structural error at each amino acid residues in the 3-D structure model. Ideally this error should be below 95% cut-off value and the residues which lie above 95% cut-off value were subjected to loop modeling in MODELLER. After each round of loop modeling, ten models were generated each of which were then further validated based on the PROCHECK and ERRAT plot. This iteration process continued until most of the amino acid residues have a cut-off value below 95% in ERRAT plot. Finally, *Leishmania* MAPK model showing the best PROCHECK and ERRAT plot was then subjected to native protein folding energy evaluation using ProsaII program [28].

Molecular dynamics study

Molecular dynamics (MD) simulations were carried out using the CHARMM [29] module in standard dynamics cascade protocol in Accelrys Discovery Studio2.0 [30]. The protein atoms were parameterized using the CHARM22 force field [31]. All bond lengths involving hydrogen atoms were fixed using SHAKE algorithm [32]. Simulations were

carried out at 300 K with 2000 steps of steepest descent and adopted basis Newton-Raphson (ABNR) minimization technique, until the root-mean square deviation (RMSD) was less than $0.001 \text{ kcal mol}^{-1} \text{ \AA}^{-1}$. The whole system was equilibrated for 50 ps, followed by another 1 ns of canonical ensemble (NVT)-MD simulation run.

Molecular electrostatic potential mapping and cavity depth analysis

Molecular electrostatic potential (MEP) and cavity depth analysis at the ATP binding pocket of *Leishmania* MAPK and human ERK2 (1TVO) were carried out using the MOLCAD program implemented in the SYBYL7.1 molecular modeling package [33]. The Gasteiger-Hückel charges were assigned to the atoms of both structures (template and target) and surfaces were generated and visualized.

The molecular electrostatic interaction is a crucial part of the non-covalent interaction energy between the molecules. The MEP on a molecular surface can be used to visually compare two molecules, guide docking studies, and identify sites that interact with its ligands. Bhattacharjee and Karle have employed the MEP technique to relate the anti-malarial potency of different carbinolamine analogs [34] with the potential values. The color ramp for the MEP ranges from deep blue color representing the most negative potential, and the deep red color representing the most positive potential, respectively.

The molecular cavity depth measures how deep a surface point is located inside the cavity of a molecule in Å. This analysis can provide the 3D spatial features of the protein-ligand interactions. The color ramp for cavity depth ranges from blue color (low depth value) to light red color (high depth value).

Molecular docking analysis

Leishmania MAPK and *Leishmania* CRK3 belong to the same protein tyrosine kinase family. As inferred from the multiple sequence alignment and 3-D structure superimposition, there is significant sequence/structure similarity of the amino acid residues at the ATP binding pocket, which in turn includes the ligand binding site of *Leishmania* MAPK, *Leishmania* CRK3 and human ERK2 proteins (Figs. 1 and 6).

Twenty ATP competing inhibitors already reported against *Leishmania* CRK3 infected macrophages *in vitro* [13], were docked against the ATP binding pocket of the 3D structure model of *Leishmania* MAPK, using FlexX and AutoDock molecular docking programs. All these ATP competing inhibitors were initially built on SYBYL7.1 and energy minimized by Powell method using Tripos force field with $0.05 \text{ kcal mol}^{-1}$ energy gradient convergence

criterion. FlexX is a fast, flexible docking method that uses an incremental construction algorithm to place ligands into the active site of the protein. *Leishmania* MAPK homology model was used for docking study. While setting docking protocol using FlexX molecular docking program, the extracted ligand was docked at the ATP binding pocket of 9.5 \AA radius in *Leishmania* MAPK model.

In order to understand the binding affinity of the ligand with the protein (*Leishmania* MAPK homology model), the most active indirubin class of molecules (**97/109**, **97/344**, **98/146**, **97/657** and **98/516**) were subjected for docking analysis using AutoDock program [35]. Docking study was performed using the Lamarckian genetic algorithm implemented in AutoDock4, which was regarded as the best docking method in terms of its ability to find the lowest energy and its structure prediction accuracy. Polar hydrogens were added using the AutoDock Tools interface. Grid maps were prepared using the AutoGrid utility with ($40 \times 48 \times 42$) points to cover the entire region occupying the active site residues of *Leishmania* MAPK homology model. Grid spacing set to 0.375 \AA . Docking parameters modified from the defaults were: number of individuals in the population (set to 150), maximum number of energy evaluations (set to 2,500,000), maximum number of generations (set to 2700), and number of genetic algorithm runs (set to 100).

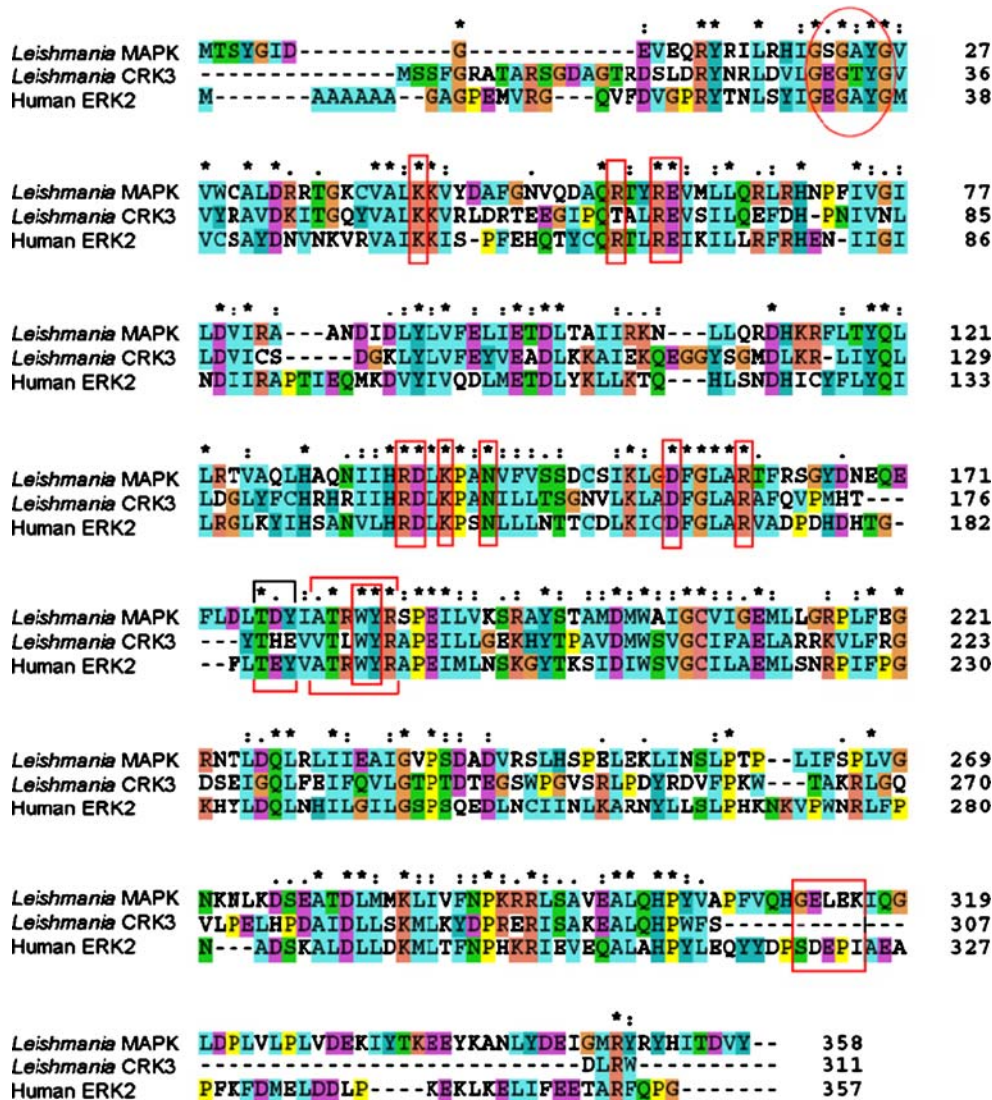
Comparative analysis of the docking results obtained using FlexX and Autodock program for indirubin class of ATP competitive LCRK3 inhibitors were performed on the *Leishmania* MAPK homology model. Furthermore, in order to understand the Ras-MAPK signal transduction pathway, the crystal structure of nuclear HDAC4 protein which is in complex with its inhibitor trifluoromethyl ketone (PDB code: 2VQJ), was subjected for docking analysis using Autodock software. HDAC4 protein is associated with the kinase activity and regulates chromatin status and gene expression. The most potent indirubin classes of molecules which are well known LCRK3 inhibitors were successfully docked in the active site of HDAC4 protein using the above mentioned docking protocol.

Results and discussion

Leishmania MAPK homology model analysis

The sequence alignment of *Leishmania* MAPK and human ERK2 (template) are shown in Fig. 1. The alignment shows that the protein kinase domain is conserved in both these MAPK homologue [4]. The human ERK2 is an extracellular signal regulated kinase 2 also called as MAPK2, has 39% sequence identity and 62% sequence similarity with the *Leishmania* MAPK.

Fig. 1 Sequence alignment of *Leishmania* MAPK with the template human ERK2 (PDB code: 1TVO) and *Leishmania* CRK3



Selection of human ERK2 as a template for the present 3D structure modeling was due to its good crystal structure resolution, and also an inhibitor present in it bears significant structural similarity to the known reported inhibitors for leishmaniasis.

The initial crude homology model structure of *Leishmania* MAPK homologue obtained from the MODELLER software was further subjected to ligand modeling. The quality of the final ligand supported *Leishmania* MAPK homology model was assessed by Ramachandran plot (in the PROCHECK validation package) and ERRAT plot. In Ramachandran plot, 86.8% of the residues were in the allowed region, 11.7% were in additionally allowed region, and 0.9% was in the generously allowed region. This indicated that the backbone dihedral angles, phi, and psi, in the *Leishmania* MAPK model were reasonably accurate. The residues in the disallowed region accounted only 0.6% of the total protein and these residues are located far away

from its different binding site residues. The model also showed good ERRAT plot (Supplementary material Fig. 1s) with the overall quality factor of 70.15%.

Finally, the quality of the protein folds of *Leishmania* MAPK homology model was evaluated using ProsaII program. In general, folding energy of the protein showed minimum value since this accounts for the stability and nativity of the molecules. ProsaII energy profile of the homology-modeled *Leishmania* MAPK in comparison to that of the X-ray structure of human ERK2 is presented in Fig. 2. The trend of the variation of the protein folding energy in most parts of the *Leishmania* MAPK model is in good agreement with that of the X-ray structure of human ERK2 protein, and is presented in Fig. 2.

In order to check the stability of the 3D structure of *Leishmania* MAPK model, MD simulation was performed. The RMSD value of *Leishmania* MAPK backbone atom is plotted as time-dependent functions of the MD simulations,

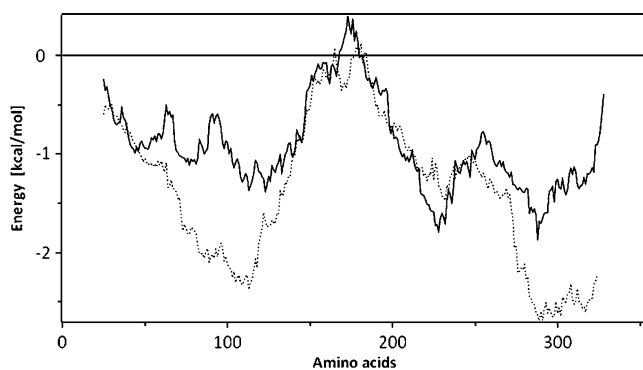


Fig. 2 ProsaiI energy profile for *Leishmania* MAPK homology model (light line) and Human ERK2 (PDB code: 1TVO) (heavy line)

and is presented in Fig. 3. The graph clearly indicates that there is a change in the RMSD from 0.3 Å to 0.7 Å in the LMAPK homology model for the first 0.3 ns and thereafter it reached a plateau. The RMSD values of the backbone atoms in the system tend to be convergent after 0.6 ns with fluctuations around 1 Å. The low RMSD and the structural comparison w.r.t. its simulation time indicates that, as expected, the 3D structure model of *Leishmania* MAPK represents a stable folding conformation.

Structure and function of *Leishmania* MAPK model

3D model structure of *Leishmania* MAPK homologue is presented in Fig. 4. The *Leishmania* MAPK is folded into the bilobal structure, a typical architecture for most of the protein kinases, with smaller N-terminal domain consisting of four antiparallel β -strands and a single α -helix. The larger C-terminal domain consisted primarily of α -helix. *Leishmania* MAPK has 12 kinase sub-domains. The kinase domain consists of nearly the entire protein starting from Tyr17 to Phe318, thus leaving only 16 residues at the N-terminal and 45 residues at the C-terminal region. Sub-domain I contained the phosphate anchor ribbon for ATP binding (GSGAYG) at the N-terminus, having consensus (GXGXXG). A conserved lysine residue (Lys43), which

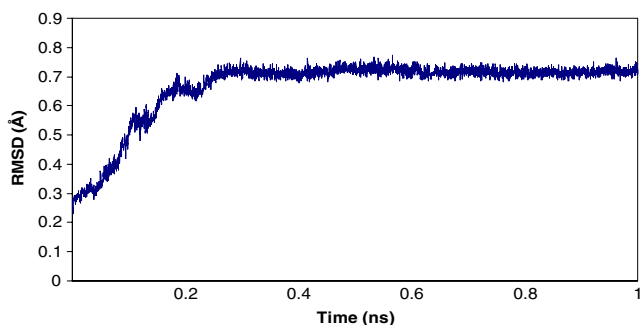


Fig. 3 Time dependence of the RMSD (Å) from *Leishmania* MAPK homology model for the backbone atoms in 1 ns MD simulation

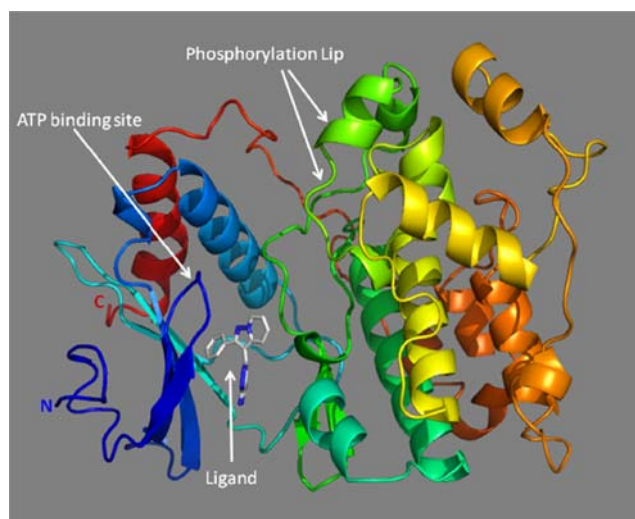


Fig. 4 3D structure model of *Leishmania* MAPK with the ligand shown in stick model

was involved in orienting the ATP for the proper phosphate reaction was located in the sub-domain II. Using site directed mutagenesis experiment, mutation of Lys43 to Met showed that the mutant form of the *Leishmania* parasite lacks autophosphorylation ability, implicating that Lys43 (numbered as Lys59 in *Leishmania mexicana* MAPK 4) is essential for its kinase activity [3, 4, 12]. The potential regulatory phosphorylation site located at sub-domain VIII, *i.e.*, Thr176 and Tyr178 in the phosphorylation lip (TXY motif) is also conserved in *Leishmania* MAPK. P+1 specificity pocket have the following residues (ATRWYR) is also well conserved in *Leishmania* MAPK and human ERK2, highlighted in Fig. 1. The common docking site region constituting (GELEK) is also important for its interaction with other proteins. Other conserved residues, a hallmarks of MAP kinases are present in the different sub-domains of these kinases [3, 4, 12]. Phosphate anchor ribbon for ATP binding site residues (GSGAYG), common docking site residues (GELEK), and catalytic site residues (KRRERDKNDR) in *Leishmania* MAPK are shown inside boxes in Fig. 1.

Using protein crystallographic method, the co-crystal structure of human ERK2 with the selective inhibitor FR180204 (PDB code: 1TVO) was solved, and structural basis of its selectivity against ERK1 and ERK2 protein was reported. The crystal structure revealed that Gln105, Asp106, Leu156, and Cys166 residues, which form the ATP-binding pocket of ERK, played an important role in the ligand-receptor interactions [26, 36].

Superimposition of the homology model of *Leishmania* MAPK and human ERK2 was reasonably good with root mean square deviation (RMSD) of 1.28 Å, which revealed overall tertiary structural similarity/differences between the two protein structures. Further superimposition at the ATP

binding pocket, *i.e.*, amino acids within 9.5 Å region surrounding ligand of *Leishmania* MAPK and human ERK2 showed good RMSD of 0.345 Å. Superimposition of amino acid residues within 3.5 Å region surrounding ligand in *Leishmania* MAPK (AKLPQIAP) and human ERK2 (AKIQKMSL) showed several important differences, and is presented in Fig. 5. In addition phosphate anchor ribbon for ATP binding amino acid residues (GSGAYG) in *Leishmania* MAPK is almost conserved (GEGAYG) in human ERK2 (Fig. 1). These relative differences/similarities in the ATP binding pocket of both these proteins should undoubtedly affect the steric and electrostatic interactions with its ATP competing inhibitors in a more specific and selective manner.

It is also well established that because of the high level of sequence homology among MAP kinases and its importance for the proliferation in the amastigotes, the protein encoded by *Leishmania* MAPK is likely to be a component of MAPK signal transduction pathway affecting cell division. This process is regulated by post-translational modification in amastigotes, and its functional activation present throughout the cell cycle is an inherent feature of the MAP kinases, being activated by phosphorylation in TXY motif by a specific MAPK kinase, and which in turn is activated by another kinase [37].

The electrostatic interaction is the main part of the interaction energy between ligands and protein, governing the strength of bonds, the strength of non-bonded interactions, and molecular reactivity. In case of a ligand-protein interaction at the active site, the ligand experiences a unique environment in terms of electrostatic, steric, and hydrophobic properties. Variations in these properties near the active site of the proteins can contribute to its selectivity/

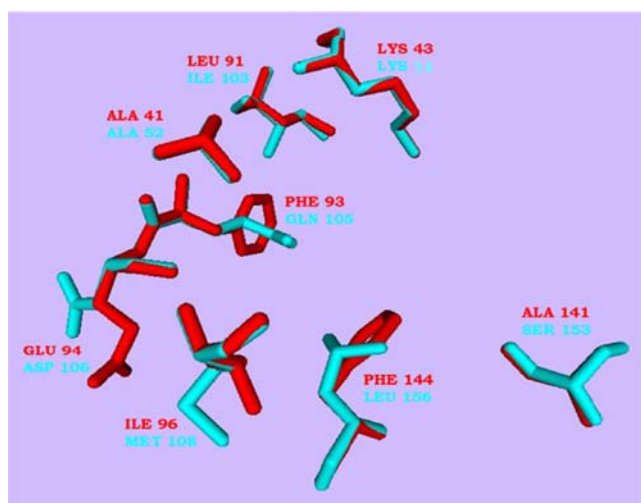


Fig. 5 Superimposition of inhibitor binding site of *Leishmania* MAPK (red) onto Human ERK2 (PDB code 1TVO) (cyan) within its 3.5 Å region

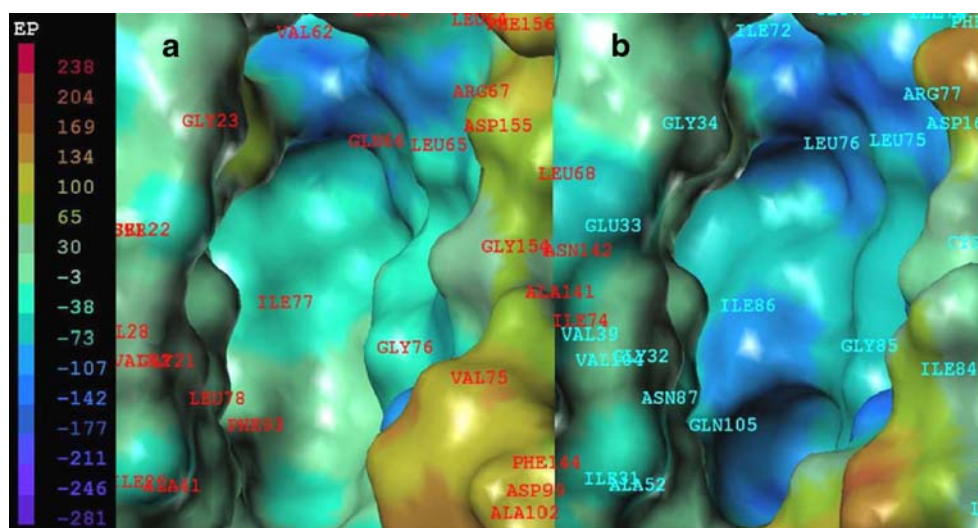
specificity. Thus comparing MEP of *Leishmania* MAPK and human ERK2 protein at the ATP binding pocket could provide an effective way for understanding selective/specific inhibition of *Leishmania* MAPK.

The MEP surface for *Leishmania* MAPK and human ERK2 are presented in Fig. 6a and b respectively, with their MEP color ramps. MEP for *Leishmania* MAPK ranging from -281 to $+239$ kcal mol $^{-1}$, while the same for human ERK2 ranging from -363 to $+182$ kcal mol $^{-1}$. In order to make comparison easier, MEP of the two proteins was placed on the same scale (-281 to $+239$ kcal mol $^{-1}$). Having placed on the same scale more specifically, comparative analysis of *Leishmania* and human ERK2 at the ATP binding pocket were carried out (Fig. 6). It was clear from Fig. 6 that the MEP covering the ATP binding pocket residues in the two proteins have different values, reflecting variation in the physico-chemical property.

Within the ATP binding pocket of *Leishmania* MAPK, the area encompassing residues Leu65, Gln66, Gly76, and Ile77 has a relatively more spread of low electronegative potential (-4 to -39 kcal mol $^{-1}$) than Lue75, Lue76, Gly85, and Ile86 residues of human ERK2 (-39 to -90 kcal mol $^{-1}$), and is presented in Fig. 6. In addition to that, contrasting feature is also visible around residues Gly76, Ile77, Phe93, and Glu94 in *Leishmania* MAPK having less electronegative potential (-4 to -39 kcal mol $^{-1}$) than corresponding residues Gly85, Ile86, Gln105, and Asp106 in human ERK2 (-73 to -108 kcal mol $^{-1}$). Furthermore, differences in MEP observed around residue Arg67 in *Leishmania* MAPK having less electronegative potential than corresponding region surrounding Arg77 in human ERK2 (Fig. 6).

The cavity depth analysis of both *Leishmania* MAPK and human ERK2 were performed and is depicted in Fig. 7. The cavity depth for *Leishmania* MAPK ranges from -0.3270 to 11 Å, while for human ERK2 this ranges from -0.3033 to 11 Å. Similar to MEP analysis, cavity depth of the *Leishmania* MAPK and human ERK2 were placed on the same scale (-0.3270 to 11 Å), followed by comparative cavity depth analysis at the ATP binding pocket (Fig. 7). In the case of *Leishmania* MAPK, area within residues Gln66, Gly76, and Ile177 has low depth value (7.2 to 8 Å) as compared to the corresponding area within residues Lue76, Gly85, and Ile186 in human ERK2, which has high depth value, *i.e.*, 10 to 11 Å. Furthermore, area encompassing residues Val75, Gly76, and Phe93 in *Leishmania* MAPK has low depth as compared to corresponding residues Ile84, Gly85, and Gln105 in human ERK2 (Fig. 7). Contrasting features are also observed for the area within residues Leu65 and Val75 in *Leishmania* MAPK having low depth as compared to Leu75 and Ile84 residues in human ERK2. These differences in the ATP binding pocket of the two

Fig. 6 Comparative molecular electrostatic potential (MEP) surface displayed for ATP binding pocket of (a) *Leishmania* MAPK and (b) human ERK2 (PDB code: 1TVO). The deep blue color represents the most negative potential, whereas the deep red color represents the most positive potential. In order to make valid comparisons between two models the electrostatic potentials have been put on the same scale



proteins can possibly make a reasonable contribution toward selective binding of substrates/inhibitors, and which in turn affect its steric and electrostatic interactions. Thus, both MEP and cavity depth analysis provided basic differences in the ATP binding pocket, which could be exploited in the future for designing *Leishmania* specific MAPK inhibitors.

Molecular docking analysis on *Leishmania* MAPK and HDAC4 protein

The molecular docking of four different classes of 20 ATP competitive inhibitors of *Leishmania* CRK3 was tested at the corresponding ATP binding site in the *Leishmania* MAPK model. Seventeen of these inhibitors displayed anti-leishmanial activity, with a 50% effective dose (ED₅₀) of less than 11 μM [13]. These molecules fell into four chemical classes: indirubins (**97/344**, **98/516**, **98/146** and **97/109**), 2,6,9-trisubstituted purines (NG56, NG58, NG64,

NG74, **NG77**, and **NG94**, including a subset of C-2-alkynylated purines, **98/126** and **98/129**), paullones (**97 N610** and **98 N217**), and derivatives of the non-specific kinase inhibitor staurosporine (**97/646**, **97/524**, and **97/647**). The paullones and staurosporine derivatives were not good inhibitors and have toxic effect on macrophages. The 2,6,9-trisubstituted purines have medium range activity and inhibited LCRK3 *in vitro* at different concentrations [13].

All 20 molecules were docked at the ATP binding pocket of *Leishmania* MAPK model, using FlexX docking program, and is presented in Table 1. Molecules belonging to the indirubin class: **98/516** and **97/344** makes strong hydrogen bonding interactions with the residues Lys43, Arg57, and Asp155 in *Leishmania* MAPK model (Table 1). These residues belong to the catalytic domain and the inhibition of which lead to impaired kinase activity [12, 13]. The hydrogen bonding interactions of molecule **98/516** with the *Leishmania* MAPK model is displayed in Fig. 8. Other amino acid residues in *Leishmania* MAPK model,

Fig. 7 Comparative cavity depth analysis displayed for ATP binding pocket of (a) *Leishmania* MAPK and (b) human ERK2 (PDB code: 1TVO). The deep yellow color indicates the highest cavity depth, whereas deep blue color the low cavity depth. In order to make valid comparisons between two models the cavity depth values have been put on the same scale

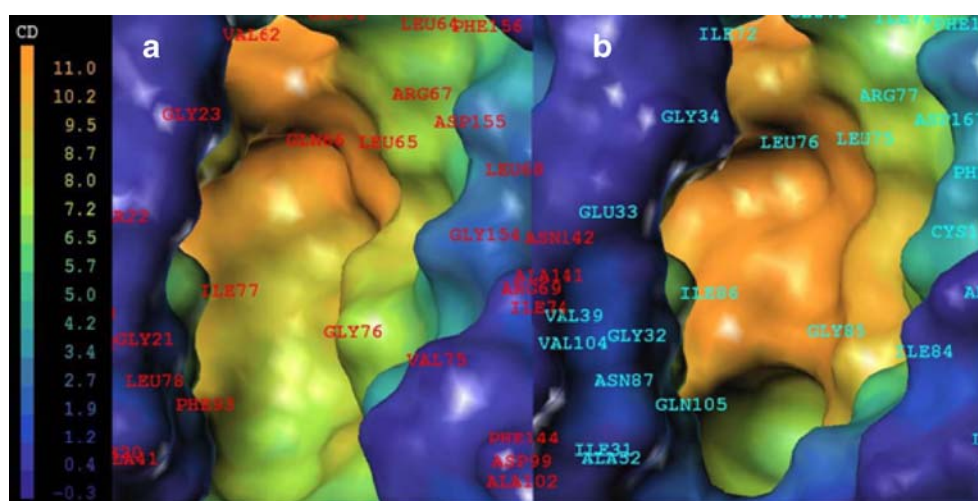


Table 1 Chemical structure, ED₅₀ (μM), FlexX and Autodock docking scores for 20 inhibitors of *Leishmania* CRK3 onto the *Leishmania* MAPK model

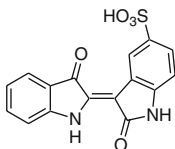
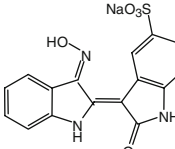
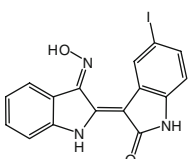
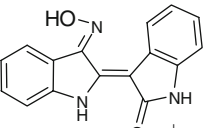
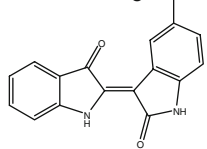
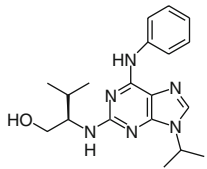
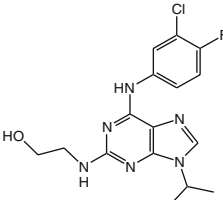
Molecule Code name	Chemical structure	^a ED ₅₀ (μM)	FlexX		Autodock		Binding residues in <i>Leishmania</i> MAPK model
			Total score	Chem. Score	Inhibition Constant Ki (μM)	Binding Energy (kcal/mol)	
Indirubins							
97/344		7.58	-27.03	-36.45	1.80	-7.84	Lys43 Arg57 Asp155
98/516		5.79	-20.67	-24.74	0.47	-8.63	Lys43 Arg57 Asp155
98/146		5.77	-21.57	-31.54	0.20	-5.07	Glu94 Ile96
97/657		>10	-20.03	-28.76	7.00	-7.03	Glu94 Ile96
97/109		8.67	-13.37	-22.38	13.79	-6.63	Ala24 Tyr25 Arg57 Asp155
Substituted Purines							
NG78		>10	-27.69	-26.31	8.21	-6.94	Ile96 Glu97 Asp99
NG64		4.76	-27.55	-26.02	11.47	-6.74	Ile96 Asp99

Table 1 (continued)

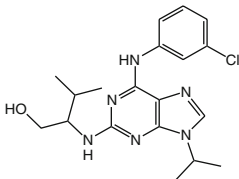
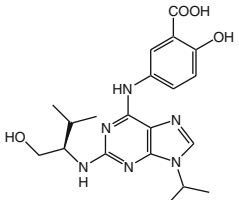
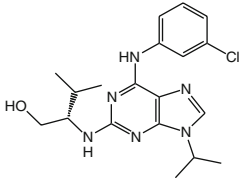
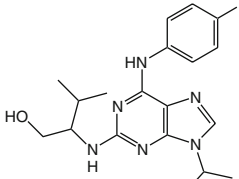
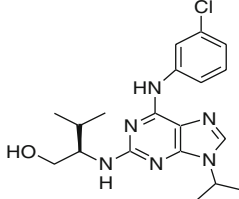
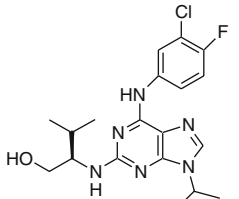
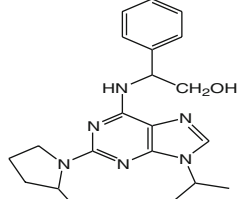
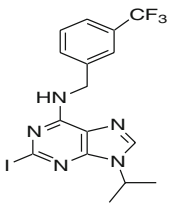
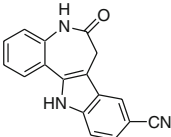
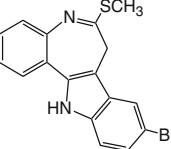
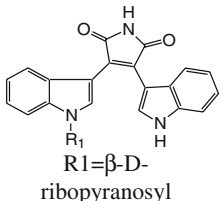
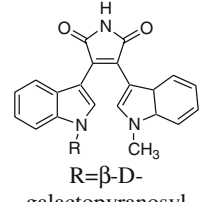
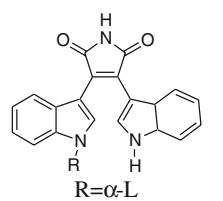
NG56		4.52	-27.51	-27.35	7.73	-6.97	Ile96 Glu97 Asp99
NG94		6.59	-26.16	-25.07	12.13	-6.71	Lys43 Arg57 Asp137 Asp155 Thr181
NG58		3.93	-22.45	-28.59	9.61	-6.84	Ile96 Glu97 Asp99
NG74		4.8	-21.34	-26.65	16.10	-6.54	Tyr25 Lys43 Glu61 Asn142
NG60		>10	-19.67	-31.49	5.76	-7.15	Lys43 Arg57 Glu61 Asp137 Lys139
NG77		9.4	-15.64	-24.80	1.40	-7.98	Tyr25 Lys43
98/126		4.04	-23.62	-26.98	2.83	-7.57	Ile96 Glu97 Ala141

Table 1 (continued)

98/129		6.66	-22.26	-23.95	79.88	-5.59	Arg18 Ile96
Paullones							
98N217		19.6	-20.46	-32.08	5.92	-7.13	Lys43 Ile96
97N610		>3	-15.64	-24.80	18.45	-6.46	Tyr25 Lys43
Staurosporines							
97/646	 R1=β-D- ribofuranosyl	5.78	-26.29	-27.59	0.12	-9.51	Ala24 Tyr25 Arg57 Asp99 Asn142
97/647	 R=β-D- galactopyranosyl	6.61	-22.16	-32.49	0.84	-8.29	Tyr25 Lys43 Arg57 Glu61
97/524	 R=α-L arabinopyranosyl	10 and 3	-32.47	-35.37	0.10	-9.54	Lys43 Lys43 Arg57 Glu61 Asp137

^aActivities of molecules tested against *Leishmania donovani*-infected macrophages *in vitro* [13]

which are involved in making hydrogen bonding interactions with the docked inhibitors include Ile96, Glu94, Glu97, Asp99, Leu95, Ala24, Tyr25, Arg18, Asn142, and Asp137 (Table 1). In order to get further insight into the binding affinity (*i.e.*, binding energy in kcal mol⁻¹ and inhibition constant in μM) of the protein and its ligand, docking analysis using Autodock program has been performed. Table 1 shows a comparative docking analysis on these 20 molecules obtained using FlexX and Autodock.

Indirubin class of four molecules showed good *in vitro* activity when tested against *Leishmania donovani* infected

macrophages. The total docking scores of these molecules were between (-13.37 to -27.03) kcal mol⁻¹ obtained using FlexX software. Using Autodock software binding energies of (-5.07 to -8.63) kcal mol⁻¹, and inhibition constants of (0.20 to 13.79) μM were obtained, and is presented in Table 1. Molecules (97/344, 98/516, 97/657, and 97/109) showed reasonably good inhibition constant and binding energy when computed using Autodock software, which is in consonance with the total score of these molecules obtained using FlexX software. A good correlation coefficient $r^2=0.87$, between *in vitro* activity and calculated binding energy was

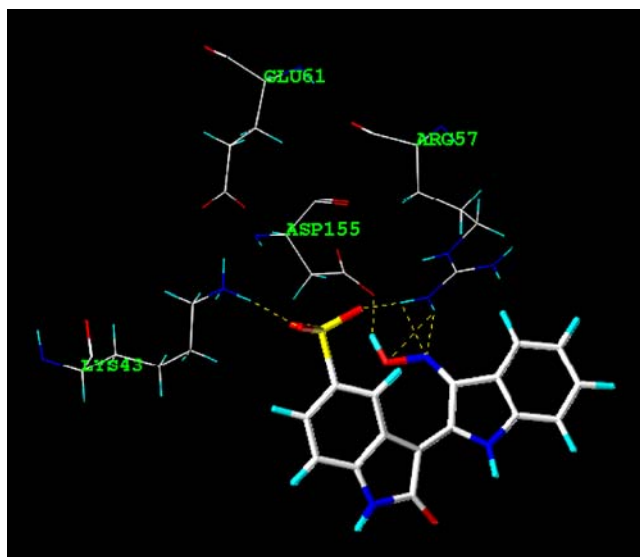


Fig. 8 Interaction of the ligand (molecule **98/516**) with the *Leishmania* MAPK 3D structure model. Hydrogen bonds are shown in yellow dotted line and ligand shown as stick model

obtained for these indirubin class of inhibitors (Table 1). Scatter plot of actual *in vitro* activities (ED_{50}) versus the binding energies computed using AutoDock software is presented in supplementary material, Fig. 2s.

Substituted purine class of eight molecules showed good *in vitro* activity when tested against *Leishmania donovani* infected macrophages. These molecules make hydrogen bonding interactions with the ATP and other binding site residues: Lys43, Arg57, Asp99, Ile96, Leu95, Glu97, Asp137, Thr181, Tyr25, Asn142, Ala141, and Arg18 (Table 1). The total docking scores of these molecules were in the range (-15.64 to -27.55) kcal mol $^{-1}$ obtained using FlexX. Using Autodock, binding energies were

obtained in the range (-5.59 to -7.98) kcal mol $^{-1}$, and inhibition constants were obtained in the range (1.40 to 79.88) μ M, and is presented in Table 1. Molecules (**NG77** and **98/126**) showed good inhibition constant and binding energy when computed using Autodock, which is contradictory with the total score obtained using FlexX (Table 1).

Paullone class of two molecules showed medium range *in vitro* activity when tested against *Leishmania donovani* infected macrophages. These molecules make hydrogen bonding interactions with the ATP and other binding site residues: Lys43, Glu97, and Ile96 (Table 1). The total docking scores of these molecules were in the range (-15.64 to -20.46) kcal mol $^{-1}$ obtained using FlexX. Using Autodock, binding energies obtained were in the range (-6.46 to -7.13) kcal mol $^{-1}$, and inhibition constants obtained were in the range (5.92 to 18.45) μ M, and is presented in Table 1. Molecules (**98 N217** and **97 N610**) showed a medium range inhibition constant and binding energy when computed using Autodock software, which is in agreement with the total score obtained using FlexX software (Table 1).

Staurosporine class of three molecules also showed medium range *in vitro* activity when tested against *Leishmania donovani* infected macrophages. These molecules make hydrogen bonding interactions with the ATP and other binding site residues: Lys43, Glu61, Ala24, Tyr25, Arg57, Asp99, and Asp137 (Table 1). The total docking scores of these molecules were between (-22.16 to -32.47) kcal mol $^{-1}$ obtained using FlexX; whereas binding energies were between (-8.29 to -9.54) kcal mol $^{-1}$, and inhibition constants were between (0.10 to 0.84) μ M, obtained using Autodock, and is presented in Table 1. The trend of variation of the inhibition constant and binding energy of these molecules obtained using Autodock software

Table 2 Docking analysis of HDAC4 protein for indirubin class of inhibitors

Molecule	ED_{50} (μ M) ^a	FlexX	Autodock		Residues involved in H-bonding of HDAC4 protein
		Total Score	Binding Energy (kcal/mol)	Inhibition Constant (K_i) μ M	
Trifluoromethyl ketone	ND	-24.04	-8.33	0.79	His159 His198
98/516	5.79	-19.05	-13.42	0.000144	His159
98/146	5.77	-16.78	-6.69	12.00	His198 Pro298
97/344	7.58	-18.36	-7.32	4.31	His198 Phe227
97/109	8.67	-14.99	-7.24	4.97	His159
97/657	10.00	-14.41	-6.03	38.31	His198 Pro298

ND- Not determined

^a Activities of molecules tested against *Leishmania donovani*-infected macrophages *in vitro* [13]

is in agreement with the total score obtained using FlexX software (Table 1). However, these classes of molecules are toxic to macrophages obtained by *in vitro* testing against *Leishmania donovani* [13].

Small molecule inhibitors are invaluable to the study of signal transduction pathways. Most known protein kinase inhibitors bind at the ATP site. High selectivity of ATP competitive binding site inhibition of indirubin and its derivatives among several CDK kinase families have been recently reported, though its mechanism of action is not yet fully elucidated. Indirubin has been used to treat chronic myelocytic leukemia which is an active ingredient of a traditional Chinese medicinal recipe, Danggui Longhui Wan [38]. It was well known that by arresting the G2/M phase of the cell cycle through inhibition of Ras MAPK pathway proteins, the *anti-proliferative* effect on the human cancer cells can be controlled [39, 40].

In order to understand the role of the MAP kinases extracellular signal regulated kinases, ERK1 and ERK2 which is in complex with HDAC4 protein, we have targeted this protein with the indirubin class of inhibitors for which the crystal structure information is available, using FlexX and Autodock program. The docking protocol was the same as described above. Five indirubin and its derivatives were successfully docked in the active site of HDAC4 protein, and are presented in Table 2. The crystal structure of HDAC4 protein in complex with trifluoromethyl ketone makes strong hydrogen bonding interactions with its active site residues, His159 and His198. As expected, indirubin and its derivatives also showed promising hydrogen bonding interactions with the His159 and His198, as well as with Phe227 and Pro298 amino acid residues. The docking score, binding energy and K_i values, of all the studied molecules obtained using FlexX and Autodock programs are presented in Table 2. Molecule **98/516** showed good inhibition constant ($0.000144 \mu\text{M}$) and binding energy ($-13.42 \text{ kcal mol}^{-1}$) obtained using Autodock in agreement with the total score (-19.05) computed using FlexX software (Table 2). It also makes hydrogen bonding interactions with the active site His159 residue of HDAC4 protein, suggesting that the docking analysis is reasonably accurate. This study showed that the indirubin class of molecules could be targeted for the inhibition of HDAC4 protein, and further *in vitro* (or *in vivo*) analysis is suggested for future development as drug like molecules in cancer therapy.

Conclusions

Homology modeling of *Leishmania* MAPK provided for the first time its 3D structure model which could be tested for screening different molecules for the *Leishmania*

specific MAPK inhibitory activity. The developed model showed good overall structural quality, and is validated using PROCHECK, ERRAT plot, and ProsaII program.

MEP surface and cavity depth analysis shows important differences in the physico-chemical properties at the ATP binding pocket of *Leishmania* MAPK and human ERK2 protein. In *Leishmania* MAPK model, low MEP and cavity depth values were observed in comparison to human ERK2 and such differences could be exploited for designing *Leishmania* specific MAPK inhibitors. Active-site modeling of the *Leishmania* parasite kinase to determine the structural differences in the ATP-binding pocket, in combination with the detail structure-activity analysis, provided clear insight on the design of the parasite-specific kinase inhibitors.

Reasonably good correlation exists between *in vitro* activity and calculated binding energy for indirubin class of inhibitors obtained from the molecular docking study. These molecules make strong hydrogen bonding interactions with Lys43, Arg57, Asp155, Glu94, and Ile96 amino acid residues of *Leishmania* MAPK model. These residues belong to the catalytic domain and the inhibition of which lead to impaired kinase activity. Thus docking analysis suggests that the indirubin class of molecules could act as putative inhibitors of *Leishmania* MAPK.

Further insight about the mode of interaction of the indirubin class of small molecules with the HDAC4 protein could provide guidance for the design of better drugs in the area of cancer disease.

Acknowledgments This research was supported by grants from the Ministry of Chemicals and Fertilizers, Govt. of India, India. CGM also acknowledges the Department of Biotechnology (IFD-Dy. No.102/IFD/SAN/ 884/2006-2009) New Delhi, India for partial financial support of this work. PS is recipient of Senior Research Fellowship from Department of Biotechnology, India.

References

1. Karioti A, Skaltsa H, Kaiser M, Tasdemir D (2009) *Phytomedicine* 16:783–787
2. Sinha PK, Pandey K, Bhattacharya SK (2005) *Indian J Med Res* 121:407–414
3. Murray HW, Berman JD, Davies CR et al. (2005) *Lancet* 366:1561–1577
4. Vazquez-Pineiro T, Fernandez AJM, Gonzalo LJC et al. (1998) *Oral Surg Oral Med Oral Pathol Oral Radiol Endod* 86:179–182
5. de MJA Garcia, Dean FA, Alamillos GF et al. (2007) *Med Oral Patol Oral Cir Bucal* 12:281–286
6. Wiese M (1998) *EMBO J* 17:2619–2628
7. Chang KP (1983) *Int Rev Cytol Suppl* 14:267–305
8. Croft SL, Coombs GH (2003) *Trends in Parasit* 19:502–508
9. Murray HW (2004) *Exp Rev Anti-infective Therapy* 2:279–292
10. Christopher SP, Kathy S, David H, Lee M et al. (2007) *Nat Genet* 39:839–847
11. Gray P, Fred R, Tara BG et al. (2001) *Endo Rev* 22(2):153–183

12. Wang Q, Melzer IM, Kruse M et al. (2005) *Kinetoplastid Biol Dise* 4:6–14
13. Grant KM, Dunion MH, Yardley V et al. (2004) *Antimicrob Agents Chemother* 48:3033–3042
14. Moon MJ, Lee SK, Lee J-W et al. (2006) *Bioorg Med Chem* 14:237–246
15. Bardwell AJ, Abdollahi M, Bardwell L (2003) *Biochem J* 370:1077–1085
16. Xianbo Z, Voctoria MR, Audrey HW et al. (2000) *Proc Natl Acad Sci* 97:14329–14333
17. Sebolt-Leopold JS (2008) *Clin Cancer Res* 14(12):3651–3666
18. Friday BB, Adjei AA (2008) *Clin Cancer Res* 14(2):342–346
19. McCubrey JA, Milella M, Tafuri A et al. (2008) *Curr Opin Investig Drugs* 9(6):614–630
20. Daouti S, Wang H, Li WH et al. (2009) *Cancer Res* 69(5):1924–1932
21. Tai K, Fowler P, Mokrab Y, Stansfeld P, Sansom MS (2008) *Methods Cell Biol* 90:233–265
22. William BH, Bisson WG, Schubiger PA, Scapozza L (2008) *J Mol Model* 14:891–899
23. Pietra F (2009) *J Chem Inf Model* 49:972–977
24. Ohori M, Kinoshita T, Okubo M et al. (2005) *Biochem Biophys Res Commun* 336:357–363
25. Marti-Renom MA, Stuart AC, Fiser A (2000) *Annu Rev Biophys Biomol Struct* 29:291–325
26. Laskowski RA, MacArthur MW, Moss DS et al. (1993) *J Appl Crystallogr* 26:283–291
27. Colovos C, Yeates TO (1993) *Protein Sci* 2:1511–1519
28. Sippl MJ (1993) *Proteins: Struct Funct Genet* 17:355–362
29. Brooks BR, Brucoleri RE, Olafson BD et al. (1983) *J Comput Chem* 4:187–217
30. DISCOVERY STUDIO, Accelrys, San Diego, CA, USA
31. MacKerell AD Jr, Bashford D, Bellott M et al. (1998) *J Phys Chem B* 102:3586–3616
32. Jean-Paul R, Giovanni C, Herman JCB (1977) *J Comput Phys* 23:327–341
33. SYBYL software package, Tripos Inc, St Louis, USA
34. Bhattacharjee AK, Karle JM (1999) *Chem Res Toxicol* 12:422–428
35. Morris GM, Goodsell DS, Halliday RS et al. (1998) *J Comput Chem* 19:1639–1662
36. Ohori M (2008) *Drug News Perspect* 21(5):245–250
37. Waskiewicz AJ, Cooper JA (1995) *Curr Opin Cell Biol* 7:798–805
38. Xiao Z, Hao Y, Liu B, Qian L (2002) *Leuk Lymphoma* 43:1763–1768
39. Hoessel R, Leclerc S, Endicott JA et al. (1999) *Nat Cell Biol* 1:60–67
40. Marko D, Schatzle S, Friedel A et al. (2001) *Br J Cancer* 84:283–289